B. E. Bates
Research Assistant.

D. E. Hardt
Assistant Professor,
Assoc. Mem. ASME

Laboratory for Manufacturing
and Productivity,
Massachusetts Institute of Technology,
Cambridge, Mass. 02139

A Real-Time Calibrated Thermal Model for Closed-Loop Weld Bead Geometry Control

A distributed source conduction model is presented as a means for prediction and control of weld width and depth. Model inputs of arc efficiency and distribution are continuously calibrated by on-line comparison of predicted topside temperatures to measured profiles, giving low errors in weld size prediction. The technique is intended for closed-loop control of MIG and TIG partial penetration welds from top-side measurements.

Introduction

The primary objective in real-time control of a fusion welding process is regulation of the weld geometry. This geometry is frequently defined by the pool width and depth. All attempts at in-process weld geometry control have dealt with accessable measurements, such as top-side width [1, 2, 3] with full penetration welds [4], or with measurement techniques that require access to the backside of the weldment [5, 6]. However, truly automated welding must control penetration (or depth) as well as top-side width. Since depth cannot be directly sensed, the aim of this work is to develop a model in a form suitable for on-line prediction and control of weld cross-sectional size based soley upon topside measurements.

Figure 1 illustrates the goal of this work. Figure 1(*a*) is an ideal two variable control system where both the weld width and depth are regulated to desired set-point values. However, since the depth cannot be directly measured, this paper presents the method outlined in Fig. 1(*b*), where an estimate of the weld depth is provided by a process model. The model runs in parallel with the actual process and is continuously calibrated on the basis of the error between a measurement of the actual top-side temperature distribution and the distribution predicted by the model. It is assumed that the weld width can measured by direct (most likely optical) methods. Thus the objectives of this research can be outlined as:

- Develop a model that suitably describes the welding process, especially with respect to puddle width and depth.
- Evaluate model accuracy by comparison of weld width, depth, area and cross-sectional profile shape with actual weld samples.
- Investigate the use of top-side width and temperature measurements for in-process calibration of the model for more accurate predictions of weld width and depth.

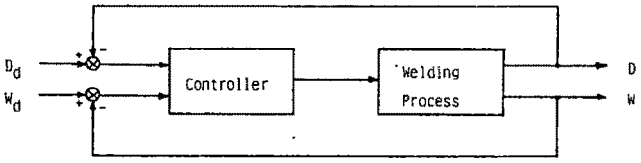

Fig. 1(*a*) An ideal two variable control system

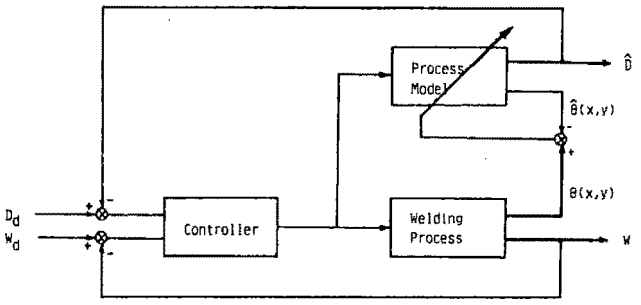

Fig. 1b Use of a Model to Provide Depth Feedback
$\theta(x,y)$ = Topside Temperature Distribution
W = Width
D = Depth

Fig. 1(*b*) The same system using a depth estimate based on a real-time calibrated model

Fig. 1 A weld pool width and depth regulator

Thermal Models of the Weld Process

Three types of models are used to describe weld puddle geometry: empirical, finite element, and analytical models. Finite element models (e.g. [7–10]), are often quite accurate but they are too slow and excessive in detail for real-time control purposes. Empirical models, such as Pavelic's fit for prediction of the top-side weld profile [11] are too inflexible for use in a control strategem, since empirical models define puddle geometry over a limited range of values for each of a set of input variables.

Contributed by the Dynamic Systems and Control Division for publication in the JOURNAL OF DYNAMIC SYSTEMS, MEASUREMENT, AND CONTROL. Manuscript received by the Dynamic Systems and Control Division, August 7, 1984.

Analytical models are considered the most promising basis for a control algorithm because they are both flexible and computationally efficient. The earliest analytical model of welding is the classic 1946 Rosenthal point source solution for temperature in the weldment [12, 13]. From a set of known input parameters (see nomenclature listing) a 3-D isotherm of melting can be produced, from which one can predict weld width, depth, and area.

Although the Rosenthal model gives a fast, qualitative understanding of the effect of input parameters on weld width and depth, it can give errors over 300 percent even if the elusive parameter arc efficiency (η) is known [14]. In addition, for on-line control of welding, efficiency will always be an unknown since it cannot be measured on a real weld. Also, weldment thermal properties are not constant, as the point source theory assumes, and since it is a pure conduction model, puddle fluid motion is also neglected. Other limitations of the model are the assumption of a single point heat source and the inability to account for unusual geometries or external conditions (such as fillet welding or the presence of heat sinks). Despite these numerous shortcomings, the major drawback of the Rosenthal model for this investigation is the fixed 1:1 half-width (W) to depth (D) ratio resulting from semi-circular isotherms. Since there is no flexibility in this aspect ratio, the basic model cannot be used to predict realistic geometries. There are, however, several modifications that can be applied to improve this aspect of the point source model.

One such modification is the standard Method of Images by which sources are placed at varying distances above and below the weldment to simulate reflections of heat back into the weldment as the top and bottom surfaces of the weldment are encountered [15]. The Method of Images then can be used to simulate the steady state thermal effect of finite thickness but can only give minor variation in the aspect ratio (W/D) as predicted by the Rosenthal model.

In 1983, Nunes [16] proposed a variation on the Rosenthal theory whereby point sources and sinks are added in a manner similar to that of the Method of Images, but at various locations within the weldment to simulate conditions such as fluid motion or heat sinks. Although the method is promising, it requires a high degree of off-line empiricism to determine appropriate sign, magnitude, and placement of the sources or sinks.

In 1980, C. L. Tsai extended the point source model to include a gaussian distributed heat source [17]. Not only is a gaussian a realistic representation of the arc heat input to the weldment [14, 15] as Fig. 2 shows, but the improved model allows for variations in pool aspect ratio (W/D). However, a new input parameter appears: arc distribution, described by the standard deviation of the gaussian (σ). Arc distribution joins arc efficiency as another unknown and unmeasurable input parameter. More recently, Eager and Tsai [14] have improved the computational efficiency of the method by reduction of the triple integral for temperature at a point to a single integral. They noted that in comparison to sectioned welds, the model can predict weld W and D with under 30 percent error, if supplied with the actual arc efficiency and distribution.

We have chosen this distributed source model as the most likely candidate for use in a control algorithm because it is well developed and reasonably accurate, does not depend greatly on off-line empirical data, and allows for variation in aspect ratio.

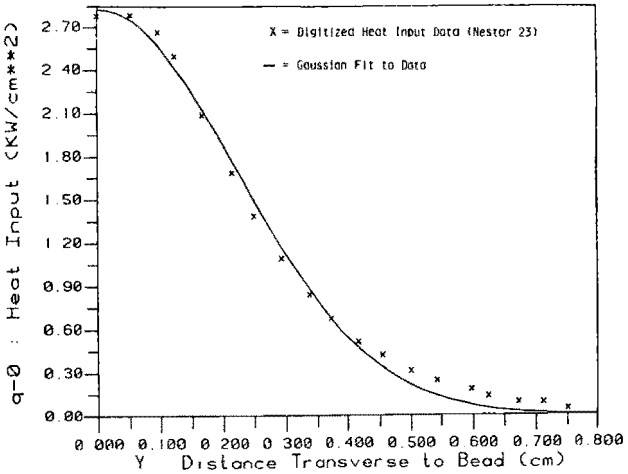

Fig. 2 A Gaussian curve fit to heat input data

Actual Torch Parameter Determination

Arc efficiency and distribution have a strong effect on scale and distribution of temperatures in the weldment and the distrubuted source model cannot be implemented without careful attention to their values. Arc efficiency (η) and distribution (σ) can be measured by applying calorimetric methods to a split anode configuration, but this is not possible for real-time control purposes. Instead, we suggest the use of an empirical relationship between (η, σ) and welding conditions from which an on-line calibration can proceed.

Arc efficiency and distribution are functions the input parameters that causally preceed arc formation and so affect the arc directly. Thus:

$$(\eta, \sigma) = f(E, I, V, \text{TIP}, \text{IP})$$

Note that arc length (L) is not included in this list since it is assured that arc length and voltage are not independent quantities [9, 18].

In the literature there is some tabulation of efficiency as a function of input parameters [19]. These findings can be separated into two bands: one group finds over 90 percent of emitted arc power received by the weldment [20, 21] while another finds much lower efficiencies of the order 35 to 65 percent [14, 19, 22]. Simple fits have been presented by researchers for η as a function of major input parameters for the higher group of efficiencies [20, 21] as well as for the lower band [14].

For this research the arc heat distribution (σ) as a function of input parameters was derived from graphs of transverse heat input distribution [23-26]. Fifty-two graphs of $q-0$ versus Y were enlarged and digitized and then for each graph, the points were fit (using [27]) to a gaussian from which was extracted. An estimate for the torch efficiency was also obtained by numerically integrating the digitized data to find the

Nomenclature

E = voltage, (11.6 volts)
I = current, (85 amps)
V = velocity, (.1668 cm/s)
IP = Ionization potential of gas, (15.76 e.v.)
TIP = electrode tip included angle, (60 degrees)
α = thermal diffusivity, (.051^2 cm/s)
k = thermal conductivity, (5.4 Btu/s-cm-F)
Tc = melting point, (1515 C)
T_0 = preheat temperature (28 C)
G = plate thickness, (.685 cm)
X = X-coordinate, (cm)
Y = Y-coordinate, (cm)
Z = Z-coordinate (cm)
L = arc length (cm)
σ = arc distribution (cm)
η = arc efficiency, (%/100)
t = time (s)

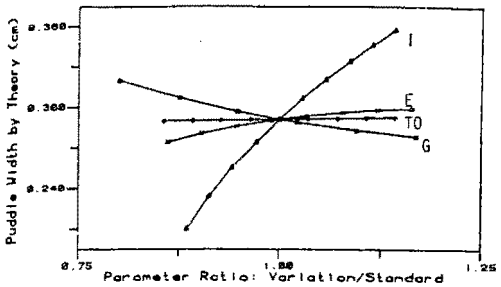

Fig. 3 Theoretical parameter effect on weld: width (standards: I = 85 amp, E = 11.6 v, T_0 = 29C, G = .685 cm)

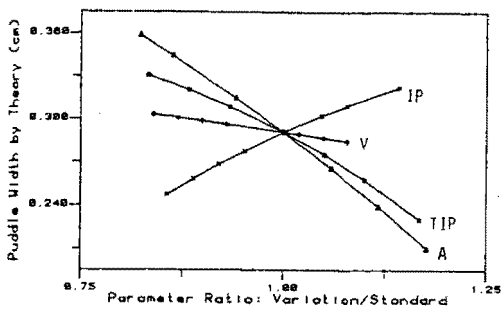

Fig. 4 Theoretical parameter effect on weld: width (standards: IP = 15.76e.v., V = .1668 cm/s, TIP = 60 deg, α = .051 cm^2/s)

total heat input to the weldment and comparing it to the power loss at the electrode. Values of σ were found on the order of 0.2 – 0.4 cm while η was consistently under 60 percent. This gave credence to the values of Niles and Jackson [19]. We used both sets of efficiency data in our curve fit for η.

Similar algebraic functions were used as the base for data fits for both arc efficiency and distribution (see [18] for details). A large number of terms were used to improve the quality of the fit. Again we emphasize that the use of such fit is as a rough starting point for on-line model calibration. However, the initial use of the fits was to test the accuracy of the uncalibrated model using this data alone.

The Uncalibrated Distributed Source Model

In practice the distributed source model can be reduced to a single integral for temperature at a point [14]:

$$\theta = \frac{N}{(2\pi)^{1/2}} \int_0^{1^2/(2)} \frac{\tau^{-1/2}}{(\tau + U^2)} \text{EXP} - \left(\frac{XX^2 + YY^2 + 2XX\tau + \tau^2}{2(\tau + U^2)} + \frac{ZZ^2}{2\tau} \right) d\tau$$

where

$N = QV/[4\pi\alpha^2\rho c(T_c - T_0)]$
$Q = \eta EI$
τ = Dummy variable of integration
$\theta = (T - T_0)/(Tc - T_0)$
$XX = (V/2\alpha)(X - Vt)$
$YY = (V/2\alpha)Y$
$ZZ = (V/2\alpha)Z$

Figures 3 through 6 show the effect of input parameter variation on weld size as predicted by equation (1), while Figs. 7 and 8 show parameter effect on η and σ. We present the two sets of graphs simultaneously since many input parameters influence the welding process, primarily through their effect on arc efficiency and distribution. In equation (1), it can be seen that η acts only as a scaling factor on the distributed source integral for temperature at a point without affecting thermal distribution in the weldment. Although less apparent in the model, σ affects temperature distribution with little effect on the temperature magnitude. Further, we consider the weld half-width, W, as a measure of scale while the aspect ratio, W/D, gives an idea of distribution of the weld since the weld cross-sectional profile is just the isotherm of melting. So η affects thermal scale and therefore weld scale (as reflected by the width, W) while σ controls the weld pool aspect ratio.

Current (I), voltage (E) and velocity (V) are designated primary input parameters since they have the largest effects on weld size. Increased voltage greatly increases the amount of heat passed to the weldment. While voltage changes appear to have little effect on arc efficiency (η), they directly effect the power (EI) emitted from the electrode. Thus, increased E should increase weld scale (W) somewhat and weld

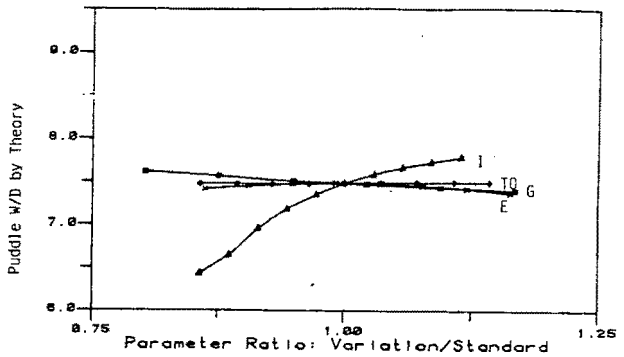

Fig. 5 Theoretical parameter effect on weld: width/depth (standards: I = 85 amp, E = 11.6 v, T_0 = 29C, G = .685 cm)

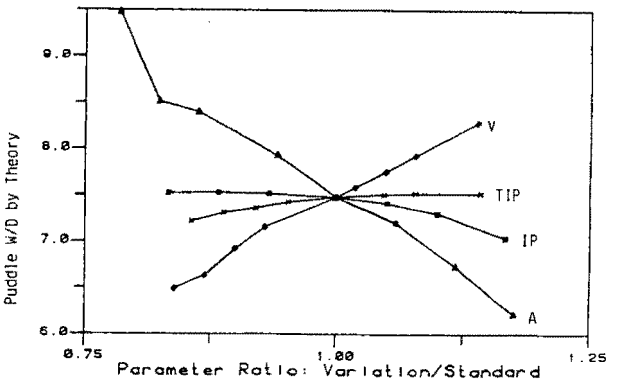

Fig. 6 Theoretical parameter effect on weld: width/depth (standards: Ip = 15.76e.v., V = .1668 cm/s, TIP = 60 deg, α = .051 cm^2/s)

distribution (W/D) greatly. The fact that the large effect on W/D isn't seen in this figure is because of the scaling. (One cannot interpret slope in the figures too directly because some parameters (like voltage) show much larger operating ranges than shown in the graphs where all parameter variations are limited to + or – 25 percent).

Increased current (I) has a scaling effect on weld size. Since Fig. 8 shows that current has little effect on σ and since current plays into the distributed source integral only as a scaling, we expect (and see) very little effect on W/D. However, increased current significantly increases the weld scale (W). This is because current (like voltage) strongly effects the emitted power so increased current will strongly raise the heat input to the weldment, even if arc efficiency is somewhat reduced.

Increased torch velocity tends to lower scale (W) and increase aspect ratio (W/D). This is largely because of the reduced heat input per unit weldment surface area; at high speeds only surface melt can occur.

Among the secondary input parameters, the material

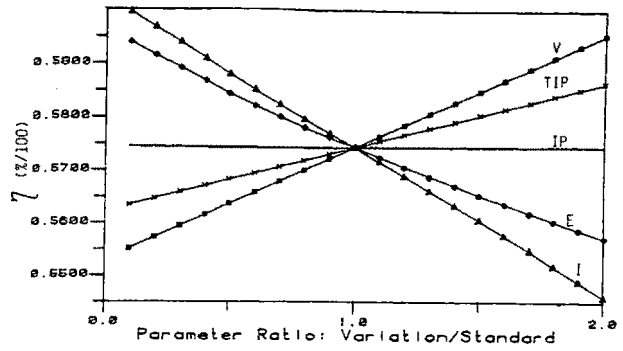

Fig. 7 Theoretical parameter effect on arc: (standards: E = 11.6v, I = 85 amp, V.1668 cm/s, TIP = 60 deg, 1P = 15.76 e.v.)

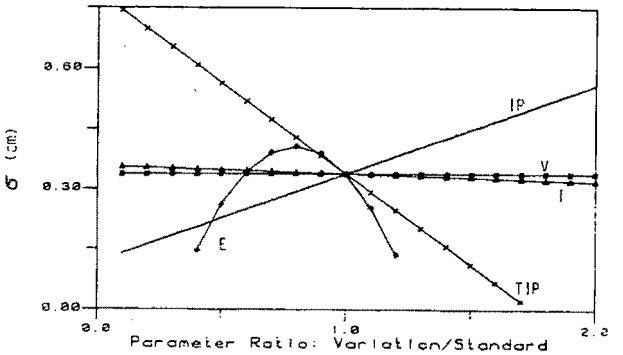

Fig. 8 Theoretical parameter effect on arc: (standards: E = 11.6 v, I = 85 amp, V = .1668 cm/s, TIP = 60 deg, 1P = 15.76 e. v.)

thermal properties are the most important. A reduction in conductivity (k) or diffusivity (α) slows Y and Z-direction heat transfer away from the point of application (i.e., the top surface of the weldment under the torch) and will tend to increase both weld scale (W) and aspect ratio (W/D). This effect will be seen to be a major shortcoming of the distributed source model since both conductivity and diffusivity fall with increased temperature.

A reduction in weldment thickness (G) also impedes heat flow, especially in the Z-direction. Below the weld pool heat flows down until it meets the bottom surface, and at steady state the Z-direction temperature gradient will drop to the point where Z-direction conduction just matches convective and radiant loss from the backside of the weldment. Clearly, an increase in D is expected as thinner plates are used, but one should also expect a rise in W as more heat is conducted away transverse to the travel direction. Figures 3 and 5 show that W rises and W/D increases slightly as G drops.

Other secondary parameters are: melting point (Tc), preheat (T_0), electrode tip angle (TIP), and gas ionization potential (IP). The melting point affects the choice of the isotherm of melting ($\theta = 1$), while percent is the baseline value ($\theta = 0$). An increase in melting point reduces weld size as the melting isotherm is moved closer to the torch while Fig. 3 shows preheat to have a slight effect on raising scale (W) by raising the baseline temperature. Shielding gas ionization potentual and electrode tip angle play into the model only by their effects on η and σ. An increase in tip angle, or a decrease in ionization potential, will increase η (and thus W) as well as σ (and therefore W/D).

Experimental Verification of Model

A series of bead on plate welds were produced to provide width and depth data for comparison with model predictions. All tests were performed using autogenous TIG on various materials of different thicknesses. The predicted puddle

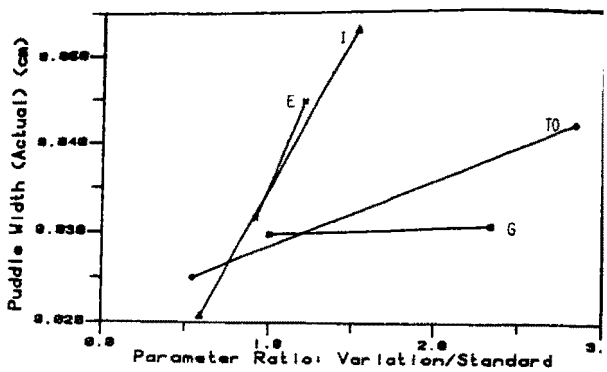

Fig. 9 Experimental parameter effect on weld: width (standards: 1 = amp, E = 11.6 v, T_0 = 29C, G = .685 cm)

width, depth, area and shape were compared to experimenta weld samples using only the rough fits described in th previous section. Input parameters were varied individuall from values set as "standards" (see captions of figures) whil all other parameters were held as close to these standar values as possible. On an average, 3 or 4 variations wer performed for each of eight input parameters (E, I, V, TIP IP, G, T_0, and Metal type) for a total of 27 sample welds Welds were laid on plates 6 in. × 10 in. in area and 1/4 in. t 1/2 in. in thickness. The welds were then sectioned, machined and ground to 600 × (20 micron) grit. The ground sample were acid-etched to highlight weld and HAZ boundaries Photographs of the samples were taken, enlarged, an digitized to give tabular Y-Z data of the weld crossection.

Figures 9 to 12 show the effect of experimental paramete variation on measured width (W) and distribution (W/D) Although we sought to vary only a single parameter at a time this often was difficult in practice. For example, changes o shielding gas (to vary ionization potential) also changed th d-c voltage levels. Also, since temperature rose quickly in ou plates, it was difficult to get an accurate measure of th preheat temperature. As a result there is some scatter on th W and W/D measurements, so a linear regression was per formed for each varied parameter.

The actual effects of parameter variation are generally th same as the model predicted. As mentioned in the previou section, increased voltage actually increases aspect ratic (W/D) strongly by increasing arc distribution while increasec current tends to reduce W/D by reducing arc distribution. Our experimental results indicate that increased tip angle tends to decrease W/D. While this is consistent with the results of Savage et al. [28], the model results show increased tip angle to slightly increase W/D.

Although the model gives good prediction of the relative effects of input parameter variation on weld quality, it does not give acceptable accuracy without modification. The scale of the predicted isotherms is generally too low and the width-to-depth ratio too high. Indeed, the standard settings that have beads on 1/4 in. mild steel plates showed no melting when input to the model (the amperage had to be raised from 85 amps to 200 amps). Eager and Tsai found that the distributed source model gives error in predicted weld width or depth of the order of 30 percent. This research found predicted temperature at the Y-Z coordinates of W and D to be up to four times below that required for melting ($\theta = 1$). Further, predicted W/D was found to be up to twice the actual, and this work showed the model to be inaccurate at high velocities (over ~ cm/s). (Some of these effects can be attributed to the infinite thickness assumption inherent in this formulation. Although our earlier work did incorporate a thickness compensation scheme based on the method of images (see Bates [18]), it was dropped because of com-

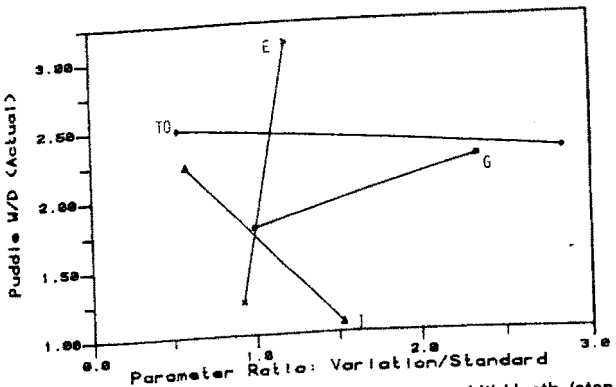

Fig. 10 Experimental parameter effect on weld: width/depth (standards: 1P = 15.76 e.v., V = .1668 cm/s, TIP 60 deg, $\alpha = .051$ cm^2/s)

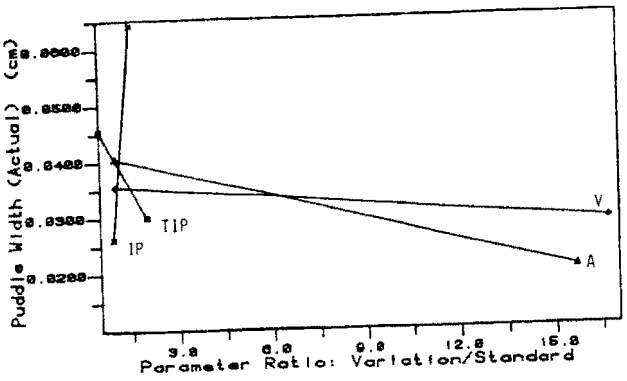

Fig. 11 Experimental parameter effect on weld: width (standards: 1 = 85 amp, E = 11.6 v, T_0 = 29C, G = .685 cm)

putational difficulties in isotherm location. However, there is no inherent reason that this cannot be reintroduced.)

It was mentioned earlier that two groups of torch efficiency values were presented in the literature. The lower efficiency set (~ 55 percent) was used in finding the results reported above. One could argue that the larger set of values might close the gap between model prediction and actual weld size. However, recall that η is largely a scaling factor whereas aspect ratio (W/D) prediction is also poor. This means that real values of both η and σ are different from those which would give real W and W/D. The argument over the proper set of efficiency values to take is thus moot. Assumption of the other set of η's would not make the model give sufficiently accurate predictions of W/D.

Of course the distributed source conduction model fails to account for fluid motion effects, and puddle convection will tend to make for larger scale of welds. Figures 10 and 12 suggest that the constant diffusivity assumption may also be an important failing of the model. As the plate heats, k and α drop, causing heat to build up near its point of application to the plate (i.e., on the top surface, near the torch). This should cause increased scale of melting (W), although the increase in W/D it could be expected to produce is not seen.

Temperature Feedback for Model Improvement

The simple distributed source model using off-line calibration is too inaccurate for use in a weld quality control strategy. For real values of η and σ the model overpredicts aspect ratio (W/D) while predicting low temperature values in general. However, if it is accepted that for some (possibly arbitrary) values of η and σ the model can predict accurate isotherms, the problem reduces to finding an on-line method for determining these "optimal" η and σ. This implies that η and σ are now simply adjustable empirical constants — stripped of their strict physical interpretation. These torch parameters now act to offset intrinsic model weaknesses (i.e., — the failure to account for non-constant thermal properties or puddle convection or phase change). It is postulated that readily accessible top-side temperature profiles can be used to direct the model to these η and σ values in real time from a curve fit initial estimate based on the empirical relationship established earlier.

Logical justification for temperature feedback is based on the fact that weld width and depth are actually end-points of the melting temperature isotherm. If the model can accurately predict top-side temperatures on the cross-section of the plate (see Fig. 13), then the weld width, occurring on the top-side ($Z = 0$) where $\theta = 1$, will automatically be accurately predicted. One would expect temperature feedback to improve depth prediction since isotherm prediction throughout the plate should be improved somewhat and one end of all isotherms (the $Z = 0$ point) will be forced to the correct location.

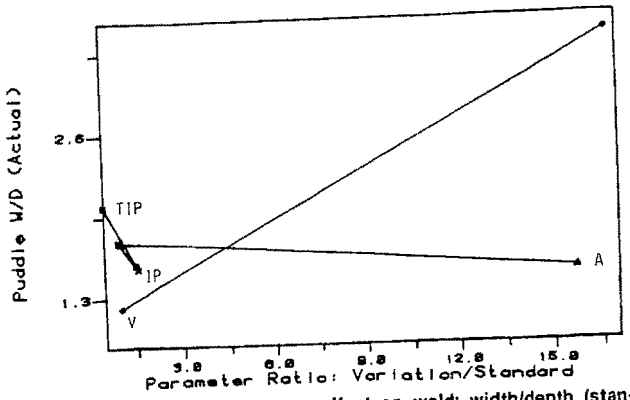

Fig. 12 Experimental parameter effect on weld: width/depth (standards: 1P = 15.76 e.v., V = .1668 cm/s, TIP = 60 deg, $\alpha = .051$ cm^2/s)

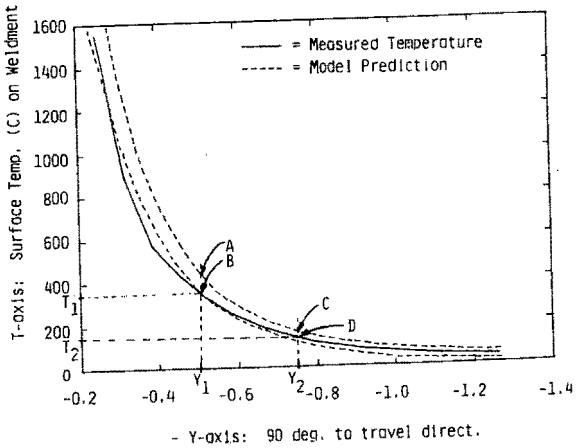

(a) Initial estimate, (b) estimate scaled to match measurement (c) $T_{\frac{1}{2}}$, (d) scaled temperatures are compared for next estimate

Fig. 13 Top-side temperature search schematic.

Arc Efficiency-Distribution Coupling. For a simultaneous search for optimal η and σ to be practicable in an on-line control algorithm, η and σ must have largely uncoupled effects on temperature scale and distribution. The uncoupling of η from temperature distribution is most apparent on the top-side. To show the effect of pure scaling vs top-side temperature profile distribution shifts, the equations given below were applied to the top-side profiles resulting from varied η and σ.

$$\text{Scaling Integral: } IA(\eta,\sigma) = \int_0^\infty \theta(Y)dY \qquad (2)$$

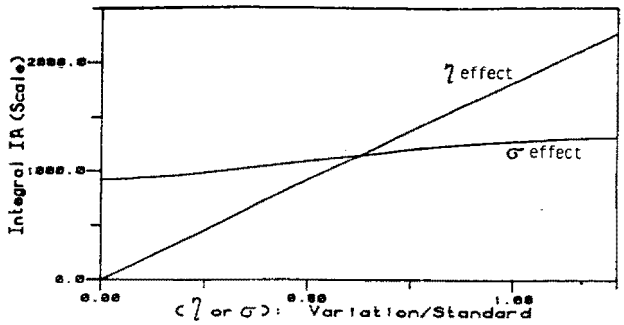

Fig. 14 (η, σ) versus top-side temperature integral: IA (scale)

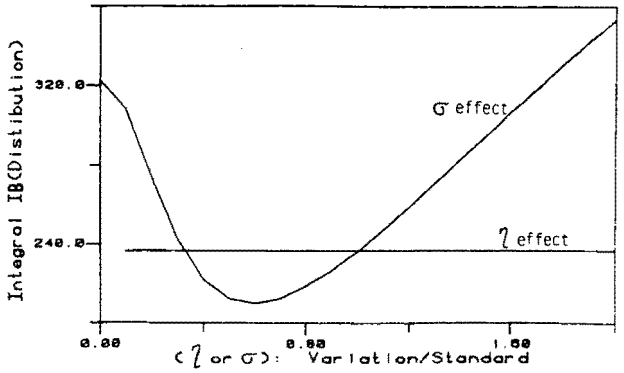

Fig. 15 (η, σ) versus top-side temperature integral: IB (distribution)

$$\text{Distribution Integral: } IB(\eta,\sigma) = \int_0^\infty \theta(Y)/\theta(Y_0)dY \qquad (3)$$

Where:

Y = Transverse distance from travel direction (here for $Z=0$)

Y_0 = Y-position at which normalizing temperature is taken

$\theta(Y)$ = Dimensionless temperature at transverse distance Y

The simpler integral, IA, gives a measure of the magnitude of top-side temperatures. The normalized equation for IB removes scaling by dividing all temperatures by a temperature midway along the Y-axis; if a temperature profile is merely scaled upward with the same shape, it will show no change in the results of IB, the distribution integral. Here, the standard parameters were again used (with I = 85 amps) while η and σ were varied from standard values (the actual η and σ fit mentioned previously). Figure 14 shows that although η has the largest effect on top-side temperature scale, σ also has a minor effect. But the near-horizontal line for η vs the distribution integral in Fig. 15 shows η is only a scaling factor on topside temperatures, as is clear from examination of the distributed source integral. Note that the top-side temperature profile distribution is controlled only by σ. It is an important benefit for an algorithm to have an uncoupled approach to finding an (η, σ) pair which predict real (W, W/D).

Optimal η, σ Search. The essential uncoupling is a boon to optimization for the η and σ pair which give real W and W/D. The main effects of increased σ increases W/D while increased η increases scale. If totally uncoupled, the search routine then can be outlined as follows:

1.) Search for σ giving proper W/D.
2.) Scale the isotherm properly by adjusting η.

Since there is still a very light coupling, the process must be repeated to accurately approach suitable settings of artificial torch parameters.

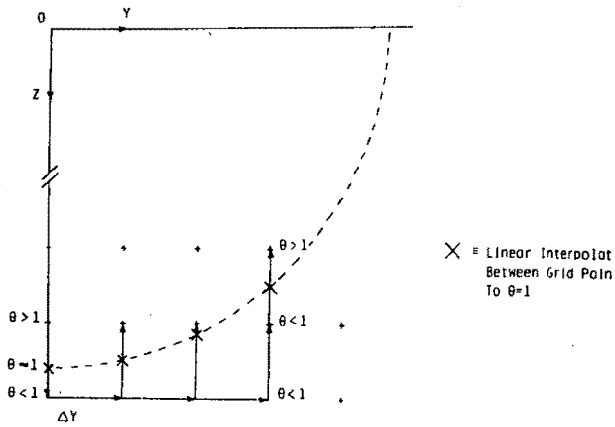

Fig. 16 Schematic of cross-sectional profile search

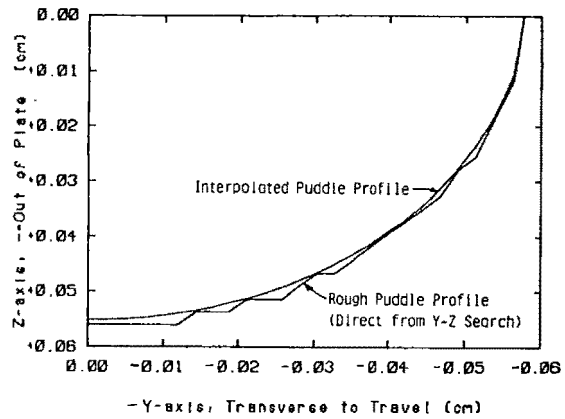

Fig. 17 Smoothing effect of linear interpolation on cross-section profile

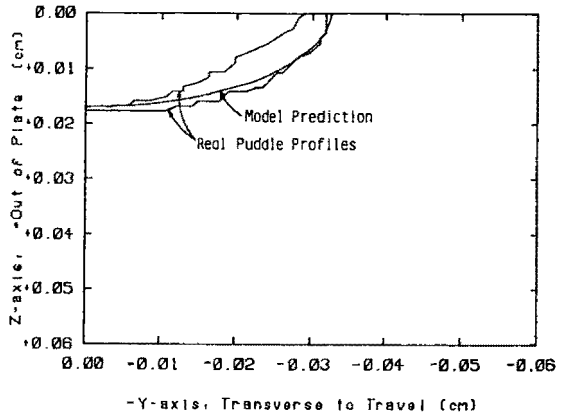

Fig. 18 Experimental versus theoretical weld cross-sections (exampl # 1)

Accuracy of the Distributed Source Model With Optima η-σ Inputs. A computer search was conducted to find wha values of η and σ could elicit the weld widths and depth found experimentally in the etched samples. The searcl algorithm is simple: given input parameters (current, voltage etc.) and the resulting weld width and depth, the progran searches for an appropriate value using the general rule tha increased σ increases W/D. Scale is then tuned by adjusting since increased η generally increases weld width (W). Becaus of the light coupling discussed above, this procedure i repeated until values of η and σ are obtained that given W an W/D within acceptable limits.

Using the such a search program predicted W and D wer

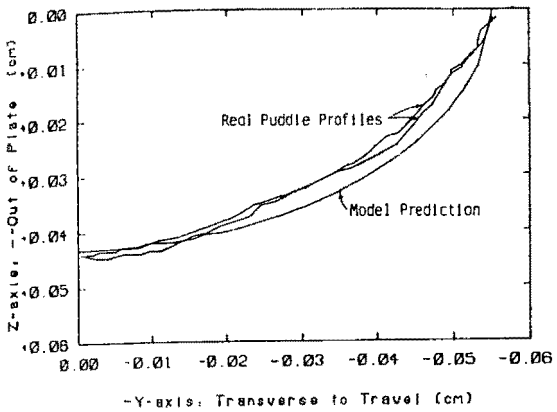

Fig. 19 Experimental versus theoretical weld cross-sections (example #2)

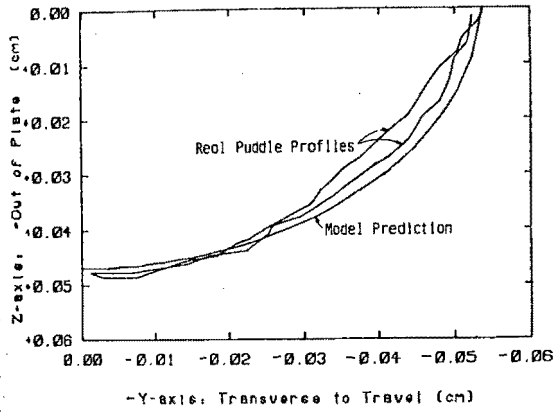

Fig. 20 Experimental versus theoretical weld cross-sections (example #3)

brought within 0.25 percent on W (or D) and 3 percent on W/D. The comparatively high error in aspect ratio was because there is some coupling between η and distribution and the search program found proper scale last. This caused some wander from the proper W/D found by the σ search.

Evaluation of the ability of the model to predict puddle area and shape requires a means of plotting the predicted cross-section – or rather the half-cross-section since the model will predict a puddle symmetric about the Z-axis. Figure 16 shows a simple search and linear interpolation graphically which:

1. Divides the Y-Z cross-section into a grid.
2. Searches down until the temperature falls below $\theta = 1$ at $Y = 0$.
3. Linearly interpolates between grid points to get puddle depth (D).
4. Moves out one Y-increment
5. Searches up one Z-increment until $\theta = 1$ is again bracketted and interpolates for the next (Y, Z) coordinates of melting.
6. Repeats steps 2 through 5 until $Z = 0$ is reached having $\theta < 1$.
7. Linearly interpolates between this (Y,0) pair and the pair one grid division closer to the origin to get W: the puddle width.

Figure 17 shows the effect of the linear interpolation, smoothing the rough search routine and giving higher accuracy. Figures 18, 19, and 20 show typical graphs of the interpolated model half-contour (using only one source image) versus the actual contour, which has been folded over onto one graph. Using the optimal (η, σ) pair found in the

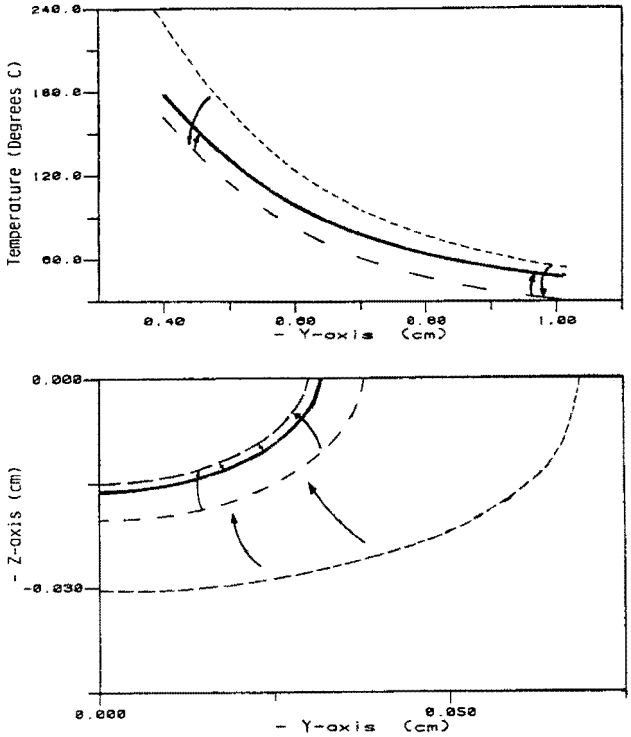

Fig. 21 Typical top-side temperaure and weld profile search (example #1)

previous section, the model tends to overpredict weld area by an average of 5 to 8 percent. The reader can qualitatively compare weld shape prediction to the actual weldment using Figs. 18 through 20. The figures show why the model overpredicts weld area. Near the puddle edge (i.e., near the puddle width) the predicted profile is not as shallow as the actual weld contour.

Optimal η-σ Curve Fits. Curve fits, similar in form to the η and σ values derived from the literature, can be constructed for optimal torch parameters as a function of input parameters. These curve fits can be used to get a rough idea of appropriate initial values of η and σ for real-time use of the model, which will give a close idea of the actual W and W/D that a set of input parameters such as current, voltage, velocity, etc. will produce.

The Use of Temperature for Torch Parameter Tuning

The curve fits above can only give initial values in the search for the (η, σ) pair needed to give the proper W and W/D. This fit alone gives high errors: over the range of parameter variations, predicted depths can be twice as high as experimental values and W/D about 1.25 times experimental aspect ratios. The aim then is to compare real top-side temperature profiles to model-predicted profiles to fine tune the input torch parameters to the model.

It is thought that the best choice for the orientation of the temperature strip is along the Y-axis, perpendicular to the direction of travel, and for convenience, at the same small X-displacement behind the torch at which the model cross-section is to be taken. This takes the temperature comparison far away from the joint where thermal distortion will occur, while allowing the strip to be taken fairly close to the origin. Further, in an experimental construction, the puddle width might even be found from topside temperature alone if the temperature strip was extended to include a small part of the puddle as well as about 1-2 cm in the solid metal beyond the weld.

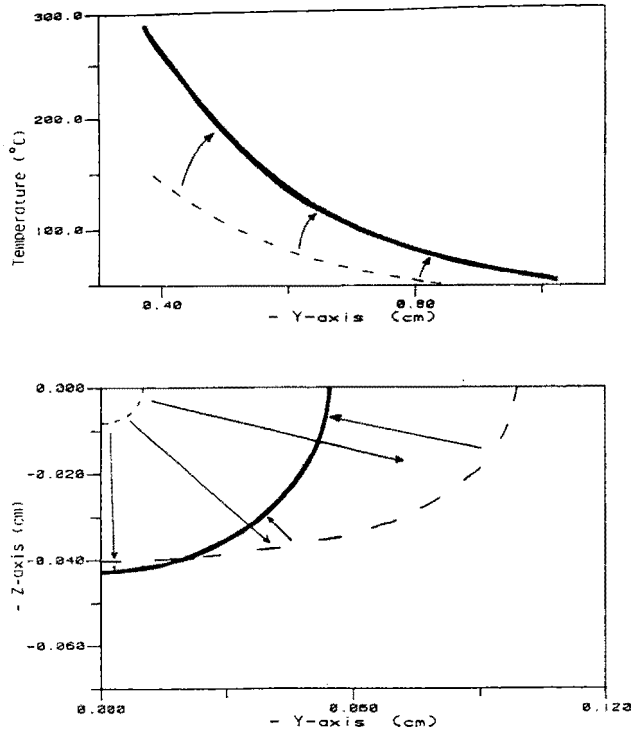

Fig. 22 Typical top-side temperaure and weld profile search (example # 2)

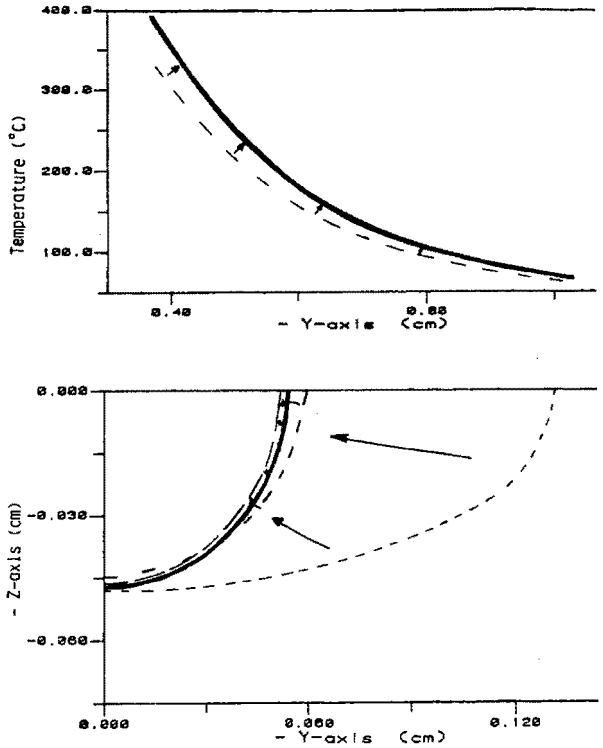

Fig. 21 Typical top-side temperaure and weld profile search (exam # 3)

Temperature Profile Comparison. The top-side temperature strip can be compared to model predicted temperature in a manner very similar to that outlined for search of η and σ using known weld W and D. A minimum of only two points on the temperature curve need be compared to the real top-side isotherm for convergence to the proper optimal η and σ. Figure 13 will assist in the explanation of the algorithm. The temperature of the leftmost point, T1*, is scaled up by a multiplicative factor so that it equals the real temperature at that point, T1. Efficiency, η, for the next loop is scaled by the same factor. The outer temperature, T2*, is scaled by the same factor as well and then is compared with the measured temperature, T2, at Y2. This comparison is used to tell whether σ is too high or too low (if the model predicts low then σ is also too low). The search routine is then a one step loop (no separate step for η adjustment, just relate scale to η) where the lowest overshoot and highest undershoot bound new choices of σ. The algorithm, can be outlined as follows:

1. Measure: the real top-side temperature profile, T-real (Y)
2. Guess: an initial (η, σ) or use the curve fits
3. Calculate: the model temperature profile, T-model (Y) for the same (Y, Z) and the same parameters
4. Scale: all model temperatures and η by: [T-real/T-model] of the innermost-Y point of the profile.
5. Integrate: the temperature difference: [T-model - T-real] accross the entire profile.
6. Search: by altering σ and returning to Step 3 until the integration in Step 5 is small and within User-set limits (η-search loop)
7. Final σ-Search: by altering σ and returning to Step 3 until the bounds on σ are small and within User-set limits (σ-search loop)

Figures 21 to 23 shows the convergence to optimal η and σ from curve fit values for the same samples shown in Figs. 18 through 20. The puddle contour and top-side temperature profile corresponding to a particular set of torch paramet (and the "standard" parameter settings) is shown in hea outline. The initial rough estimates given by the optimal cu fit are shown in the lightest shade. Convergence is shown increasingly darker shades. Convergence within 1 percent the set W and W/D can be gotten in 10 to 20 iterations, thu way of predicting actual weld cross-sectional width, depth a area from theoretical top-side temperature information h been found.

Discussion

In this work, the Distributed Source conduction model C. L. Tsai [11] is chosen as the most promising model for t in closed-loop control of an automated welder. T distributed heat source is not only a very realistic repres tation of the torch input but also allows variations in W ratio which the classic Rosenthal point source model will n As an analytic model, as opposed to a finite element model fast algorithm suitable for can be obtained. Values of tor parameters from the literature range from .35 to .65 for 7 a .2 to .4 cm for 6. However, these values give low theoreti temperatures when compared to experimental wel Although Eager and Tsai [14] found a maximum of 30 perc error in prediction of weld width and depth, this work fir predicted temperatures below melting in all of 27 ca (generally under 1/4 of the melting temperature) whi produce real welds and high aspect ratios of predict isotherms (W/D of the isotherm passing through (0, G/2) an average of 1.96 times too high, with a maximum error 3.5 times and minimum of 0.93 times).

However, values of η and σ can be chosen to give the re values of weld W and D. The effects of η and σ are large decoupled such that η affects puddle scale while σ affe aspect ratio. An off-line search can be conducted to obtain t "optimal" (η, σ) pair for a given set of input paramete (current, voltage, velocity, etc.) and known weld W and D (W and W/D). When performed on the 27 samples, there w less than 0.2 percent error on W (scale) but up to 3 perce error on W/D (puddle distribution). This is because the e

fects of η as pure scale and σ as pure distribution are not completely decoupled. Although variations as large as 2.5 times were seen, on average puddle area was over-predicted by an average of 5 to 8 percent. The over-prediction of weld area s partly due to over-predicted weld width and depth but also due in part to errors in the predicted puddle shape; the predicted puddle cross-section is not shallow enough near the puddle width.

An optimal curve fit for (η, σ) as a function of input parameters was found as a rough starting point for "optimal" torch parameter determination. The fit gives W/D ratios up o 1.5 times too high and W up to 2.0 times too high.

From this rough fit the torch parameters can be driven to he optimal values by forcing the model to predict the correct op-side temperature. A model-predicted temperature strip is compared to the real plate temperature (in this case only a arget theoretical strip of known η and σ was used) and the orch parameters were updated using the η-temperature scale nd σ-temperature distribution analogy. Because of the aforementioned decoupling advantages, the on-line temperature feedback algorithm is faster and more accurate than he off-line weld W and W/D search. Using temperature eedback, errors in W and W/D under 1 percent can be obained in 10 to 20 iterations with time of calculation being the nly drawback to even higher accuracies.

Although the applicability of this model to diverse rocesses and materials is not guaranteed, it must be emphasized that the temperature profile convergence scheme is based on matching the predicted *solid-phase* isotherms. Thus certain (as yet undetermined) degree of independence from mass transfer and fluid motion effects can be expected.

Conclusions

A means by which weld geometry (weld width and depth) an be determined using known input weld parameters and op-side temperature has been developed. Comparison of redicted to real temperature is the means by which the model forced to remain a faithful representation of the weld rocess. However, the "target" temperature profile used in his work were theoretically determined; there is as yet no uarantee that real temperature profiles look like those used. f they do not look alike then the temperature feedback lgorithm may not be useful.

Although previous work indicates that the weld plant has a ng time constant [22], the speed of the algorithm is still a onsideration. If real top-side temperature measurements stify further work, the algorithm should be streamlined, ith consideration paid to the speed of basic operations.

References

1 Richardson, R. W., Gutow, D. A., and Rao, S. H., "A Vision Based System for Arc Weld Pool Size Control," *Measurement and Control for Batch Manufacturing*, Hardt, ed., ASME, New York, 1982.

2 Sweet, L. M., Case, A. W., Corby, N. R., Kuchar, N. R., "Closed-Loop Joint Tracking, Puddle Centering, and Weld Process Control Using and Integrated Weld Torch Vision System," *Control of Manufacturing Processes and Robotic Systems*, Hardt and Book, eds., ASME, New York, 1983, pp. 107-119.

3 Vroman, A. R., and Brandt, H., "Feedback Control of GTA Welding Using Puddle Width Measurement," *Welding Journal*, Sept. 1976, pp. 742-749.

4 Zacksenhouse, M., and Hardt, D. E., "Weld Pool Impedance Identification for Size Measurement and Control," ASME JOURNAL OF DYNAMIC SYSTEMS, MEASUREMENT AND CONTROL, Vol. 105, No. 4, 1983.

5 Nomura, et al., "Arc Light Intensity Controls Current in SA Welding System," *Welding and Metal Fabrication*, Sept. 1980, pp. 457-463.

6 Smith, C. J., "Self-Adaptive Control of Penetration in a Tungsten Inert Gas Weld," *Advances in Welding Processes*, The Welding Institute, 1978, pp. 272-282.

7 Dror, Y., "Calculations and Measurement of Weld Puddle Geometry in GTA Welding," S. M. Thesis, Department of Ocean Engineering, M.I.T., June 1981.

8 Karniadakis, G., S. M. Thesis, Department of Mechanical Engineering, M.I.T., June 1984.

9 Glickstein, S. S., Friedman, and Yeniscavich, W., "Investigation of Alloy 600 Welding Parameters," *Welding Journal*, Apr. 1975, pp. 113s-121s.

10 Glickstein, S. S., and Friedman, E., "Technical Note: Effect of Weld Pool Configuration on Heat Affected Zone Shape," *Welding Journal*, Vol. 60, No. 6, 1981.

11 Pavelic, V., and Tsao, K. C., "Weld Puddle Shape and Size Correlation in a Metal Plate Welded by the GTA Process," *Arc Physics and Weld Pool Behavior*, The Welding Institute, London, England, May 1979.

12 Rosenthal, D., "Mathematical Theory of Heat Distribution During Welding and Cutting," *Welding Journal*, Vol. 20, No. 5, 1941, pp. 220s-234s.

13 Rosenthal, D., "The Theory of Moving Sources of Heat and its Applications to Metal Treatment," *Trans. ASME*, Nov. 1946, pp. 849-866.

14 Tsai, N., "Heat Distribution and Weld Bead Geometry in Arc Welding," Ph.D. Thesis, Department of Materials Science, M.I.T., Apr. 1983.

15 Meyers, P. S., Uyehara, O. A., and Borman, G. L., "Fundamentals of Heat Flow in Welding," *Welding Research Council Bulletin*, No. 123, July 1967.

16 Nunes, A. C. Jr., "An Extended Rosenthal Weld Model," *Welding Journal*, June 1983, pp. 165s-170s.

17 Tsai, C. L., "Modelling of Thermal Behaviours of Metals During Welding," *Trends in Welding Research in The United States*, American Society for Metal, Metal Park, Ohio, pp. 77-89.

18 Bates, B., "Automatic GTAW Using a Distributed Arc Model for Thermal Control of Weld Puddle Geometry," S.M. Thesis, Department of Mechanical Engineering, M.I.T., June 1983.

19 Niles, R. W., and Jackson, C. E., "Weld Thermal Efficiency of the GTAW Process," *Welding Journal*, Vol. 54, No. 1, 1975, pp. 26-32s.

20 Eberhart, R. C., and Seban, "The Energy Balance for a High Current Argon Arc," *Heat and Mass Transfer*, Vol. 9, Great Britain 1966, pp. 939-949.

21 Ghent, H. W., Roberts, D. W., Hermance, C. E., Kerr, H. W., and Strong, A. B., "Arc Efficiency in TIG Welds," *Arc Physics and Weld Pool Behavior*, The Welding Institute, London, May 1979.

22 Christensen, N., Davies, V., and Gjermundsen, K., "The Distribution of Temperatures in Arc Welding," *British Welding Journal*, Vol. 12, No. 2, 1965, pp. 54-75.

23 Nestor, O. H., "Heat Intensity and Current Density Distribution at the Anode of High Current Inert Gas Arcs," *Journal of Applied Physics*, Vol. 33, No. 5, 1962, pp. 1638-1648.

24 Schoeck, P. A., "An Investigation of the Anode Energy Balance of High Intensity Arcs in Argon," *Modern Developments in Heat Transfer*, Academic Press, New York, 1963, pp. 353-478.

25 Rykalin, N. N., "Energy Source Used for Welding," *Welding in the World*, Vol. 12, No. 9/10, 1974, pp. 227-247.

26 Rykalin, N. N., and Nikolaev, A. V., "Welding Arc Heat Flow," *Welding in the World*, Vol. 9, No. 3/4, 1971, pp. 112-132.

27 Bevington, P. R., *Data Reduction and Error Analysis for the Physical Sciences*, McGraw-Hill Inc., 1969.

28 Savage, W. F., Struck, S. S., and Ishikawa, Y., "The Effect of Electrode Geometry in Gas Tungsten-Arc Welding," *Welding Journal*, Nov. 1963.